Published in final edited form as:
Nat Genet. 2010 January ; 42(1): 83–88. doi:10.1038/ng.498.

Skp2 is required for survival of aberrantly proliferating *Rb1*-deficient cells and for tumorigenesis in *Rb1*$^{+/-}$ mice

Hongbo Wang[1], **Frederick Bauzon**[1,*], **Peng Ji**[1,*], **Xiaoliang Xu**[3,*], **Daqian Sun**[1], **Joseph Locker**[2], **Rani S. Sellers**[2], **Keiko Nakayama**[4], **Keiich I. Nakayama**[5], **David Cobrinik**[3], and **Liang Zhu**[1]

[1]Department of Developmental and Molecular Biology, and Medicine, The Albert Einstein Comprehensive Cancer Center and Liver Research Center, Albert Einstein College of Medicine, Bronx, NY 10461, USA

[2]Department of Pathology, The Albert Einstein Comprehensive Cancer Center and Liver Research Center, Albert Einstein College of Medicine, Bronx, NY 10461, USA

[3]Dyson Vision Research Institute, Weill Medical College of Cornell University, New York, NY 10021

[4]Department of Functional Genomics, Division of Developmental Genetics, Tohoku University Graduate School of Medicine, Sendai 980-8575, Japan

[5]Department of Molecular and Cellular Biology, Medical Institute of Bioregulation, Kyushu University, Fukuoka 812-8582, Japan

Abstract

Heterozygosity of the retinoblastoma gene *Rb1* elicits tumorigenesis in susceptible tissues following spontaneous loss of the remaining functional allele. Inactivation of previously studied pRb targets partially inhibited tumorigenesis in *Rb1*$^{+/-}$ mice [1,2,3,4,5,6]. Here, we report that inactivation of pRb target Skp2 [7,8] completely prevents spontaneous tumorigenesis in *Rb1*$^{+/-}$ mice. Targeted *Rb1* deletion in melanotrophs ablates the entire pituitary intermediate lobe when Skp2 is inactivated. Skp2 inactivation does not inhibit aberrant proliferation of *Rb1*-deleted melanotrophs, but induces their apoptotic death. Eliminating p27 phosphorylation on T187 in p27T187A knockin mice reproduces the effects of *Skp2* knockout, identifying p27 ubiquitination by SCF^{Skp2} ubiquitin ligase as the underlying mechanism for Skp2's essential tumorigenic role in this setting. *RB1*-deficient human retinoblastoma cells also undergo apoptosis after Skp2 knockdown; and ectopic expression of p27, especially the p27T187A mutant, induces apoptosis. These results reveal that *Skp2* becomes an essential survival gene when susceptible cells incur *Rb1* deficiency.

Corresponding author: Dr. Liang Zhu, Department of Developmental and Molecular Biology, Albert Einstein College of Medicine, 1300 Morris Park Avenue, Room U-521, Bronx, NY 10461, USA, Phone: 718-430-3320, Fax: 718-430-8975, lizhu@aecom.yu.edu.
*These authors contributed equally and are listed alphabetically.
PJ's present address: Whitehead Institute for Biomedical Research, Nine Cambridge Center Cambridge, MA 02142
HW's present address: Peptide Binding Laboratory, The Salk Institute, 10010 N. Torrey Pines Rd. La Jolla, CA 92037-1099
XX's present address: Department of Pathology, Memorial Sloan-Kettering Cancer Center, New York, NY 10021
DC's present address: Sloan-Kettering Institute, Memorial Sloan-Kettering Cancer Center, New York, NY 10021

AUTHOR CONTRIBUTIONS HW, PJ, FB, DS, and LZ designed and performed experiments with mice mutant for *Rb1*, *Skp2*, *p27*, or targeted deletion of *Rb1*. JL and RS performed pathology studies. DC and XX designed and performed analyses of retinoblastoma cells; HW performed Western blot experiments. KN and KN provided *Skp2*$^{+/-}$ mice. HW, JL, DC, and LZ wrote the paper.

COMPETING INTERESTS STATEMENT The authors declare no competing financial interests.

Skp2 binds T187-phosphorylated p27 for the SCF^{Skp2} ubiquitin ligase to ubiquitinate p27[9]. pRb binds Skp2 to interfere with this binding and ubiquitination[7]. pRb-Skp2 binding also bridges Skp2 to the APC-Cdh1 ubiquitin ligase for Skp2 ubiquitination[8]. Since Skp2 is an E2F target [10,11], pRb could repress Skp2 mRNA expression via E2F. Consistent with the above findings, *Rb1*$^{+/-}$ mice developed *Rb1*$^{-/-}$ pituitary tumors that had significantly increased amounts of Skp2 mRNA and protein along with decreased amounts of p27 protein (Fig. 1ab).

To define the role of Skp2 in tumorigenesis in *Rb1*$^{+/-}$ mice, we generated cohorts of *Rb1*$^{+/-}$*Skp2*$^{+/+}$ and *Rb1*$^{+/-}$*Skp2*$^{-/-}$ mice. Skp2 is not required for pituitary gland development (see Supplemental Fig. 2). *Rb1*$^{+/-}$ mice develop pituitary intermediate lobe (IL) melanotroph tumors with a well-defined course, from early atypical proliferates (EAP) to foci, microscopic tumors, and gross tumors (Supplemental Fig. 1a), resulting in death around one year of age [12]. At 6-month, more than half of *Rb1*$^{+/-}$*Skp2*$^{+/+}$ mice had EAPs and foci (Fig. 1c). By 9 months, one pituitary had a gross tumor, while most had foci and microscopic tumors. Later, all 27 *Rb1*$^{+/-}$*Skp2*$^{+/+}$ mice died between 10 to 15 months of age (Fig. 1d), with gross pituitary tumors except for one (Fig. 1c). In contrast, none of the *Rb1*$^{+/-}$*Skp2*$^{-/-}$ mice had any sign of pituitary tumorigenesis at 6, 9, and 17 months, when healthy *Rb1*$^{+/-}$*Skp2*$^{-/-}$ mice were sacrificed.

Thyroid C-cell tumors develop with 50-70% penetrance in *Rb1*$^{+/-}$ mice. Sixteen of the same 27 *Rb1*$^{+/-}$*Skp2*$^{+/+}$ mice had gross thyroid tumors at death, and that the dead mouse that lacked a pituitary tumor had an especially large thyroid tumor (Fig. 1c). About half of the remaining dead mice had microscopic thyroid tumors (Fig. 1c and Supplemental Fig. 1b). In contrast, all 29 *Rb1*$^{+/-}$*Skp2*$^{-/-}$ mice had normal appearing tumor-free thyroid glands (Fig. 1c). Together with the lack of pituitary tumors, these results identify Skp2 as the first pRb target that is required for spontaneous tumorigenesis in *Rb1*$^{+/-}$ mice.

The above findings could reflect that Skp2 plays a required role in the development of *Rb1* mutant tumors or that Skp2 is generally required for tumorigenesis. To begin to investigate these possibilities, we treated *Skp2*$^{+/+}$ and *Skp2*$^{-/-}$ mice with an ENU-induced tumorigenesis protocol. This experiment demonstrated no difference in tumor development in the two genotypes, including survival (Fig. 1e) and tumor types and burdens (Supplemental Fig. 3a). Although Skp2 was frequently overexpressed in the tumors, its expression levels did not correlate with p27 protein levels (Supplemental Fig. 3b). Thus, Skp2 is not required for ENU-induced tumorigenesis.

Since spontaneous tumorigenesis in *Rb1*$^{+/-}$ mice requires the loss of the remaining *Rb1* allele, it was possible that *Skp2* inactivation prevented the second *Rb1* mutation, rather than the growth of *Rb1*-deficient tumors. We next used POMC-Cre and loxP-directed tissue-specific *Rb1* deletion to artificially generate *Rb1*$^{-/-}$ pituitary IL melanotrophs [13]. To determine whether *Skp2* inactivation affects the efficiency of POMC-Cre-loxP-mediated recombination, we generated POMC-Cre;Rosa26R;*Skp2*$^{+/+}$ and POMC-Cre;Rosa26R;*Skp2*$^{-/-}$ mice. Fig. 2a shows that the POMC-Cre strain could induce Cre-loxP-mediated deletion in most of the IL melanotrophs in both *Skp2*$^{+/+}$ and *Skp2*$^{-/-}$ mice. Since the POMC promoter is also active in corticotrophs in the anterior lobe (AL), scattered AL recombination events were detected in both strains of mice as well (Fig. 2a5,6).

We then generated POMC-Cre;*Rb1*$^{lox/lox}$*Skp2*$^{+/+}$ and POMC-Cre;*Rb1*$^{lox/lox}$*Skp2*$^{-/-}$ mice and examined their pituitary glands at 7 weeks of age. As expected[13], POMC-Cre;*Rb1*$^{lox/lox}$*Skp2*$^{+/+}$ mice contained dysplastic nodular lesions across the entire ILs (Fig. 2b2,6). Unexpectedly, POMC-Cre;*Rb1*$^{lox/lox}$*Skp2*$^{-/-}$ mice did not contain normal-appearing ILs as we predicted based on the lack of pituitary tumorigenesis in *Rb1*$^{+/-}$*Skp2*$^{-/-}$ mice.

Rather, the ILs of these mice were essentially absent with only a single layer of lining cells separating the anterior and posterior lobes (Fig. 2b3,7). The ILs of POMC-Cre;*Rb1*$^{lox/lox}$*Skp2*$^{+/-}$ mice were also significantly thinner than normal (Fig. 2b4,8). These results confirm that *Skp2* inactivation blocks tumorigenesis and demonstrate that this effect was achieved not by reverting *Rb1*-deficient melanotrophs to normal cells, but by eliminating them.

We traced the fate of *Rb1* and *Skp2* doubly deficient melanotrophs by generating POMC-Cre;Rosa26R;*Rb1*$^{lox/lox}$*Skp2*$^{+/+}$ and POMC-Cre;Rosa26R;*Rb1*$^{lox/lox}$*Skp2*$^{-/-}$ mice and allowing them to age to 10-13 weeks. As shown in Fig. 2c1,3, the ILs of POMC-Cre;Rosa26R;*Rb1*$^{lox/lox}$*Skp2*$^{+/+}$ mice, observed with hematoxylin stain and EYFP fluorescence, were in more advanced stages of tumorigenesis than those at 7 weeks (compare with Fig. 2b2), whereas the ILs of POMC-Cre;Rosa26R;*Rb1*$^{lox/lox}$*Skp2*$^{-/-}$ mice remained a single-cell layer (Fig. 2c2). Interestingly, the cells in this layer were EYFP positive (Fig. 2c4), suggesting that this single-cell layer environment could prevent death of *Rb1* and *Skp2* doubly deficient cells or that these cells escaped *Rb1* deletion. We also found that *Rb1* deletion in corticotrophs induced the presence of more corticotrophs in the AL, and combined deletion of *Rb1* and *Skp2* dramatically reduced their numbers (Fig. 2a5,6 and 2c3,4). This indicates that combined *Rb1* and *Skp2* deletion could eliminate corticotrophs as well as melanotrophs.

We next harvested the mice at earlier ages to investigate how the ILs were eliminated. At post natal day (PND) 10, the ILs of both POMC-Cre;*Rb1*$^{lox/lox}$*Skp2*$^{+/+}$ and POMC-Cre;*Rb1*$^{lox/lox}$*Skp2*$^{-/-}$ mice showed slightly higher cellularity compared with that of *Rb1*$^{lox/lox}$ mice (Fig. 3a1,6,11 and data not shown). Expression of PCNA (an E2F target gene) and Ki67 (a proliferation marker) was readily observed in *Rb1*$^{lox/lox}$ melanotrophs indicating the proliferative status of these cells at this age (Fig. 3a2,3 and c). Deletion of *Rb1* increased PCNA and Ki67 expression, consistent with deregulation of E2F and proliferation caused by pRb inactivation (Fig. 3a7,8 and c). *Skp2* inactivation did not reduce PCNA expression nor the aberrant proliferation of the *Rb1*-deficient cells (Fig. 3a12,13 and c), but significantly increased TUNEL positive IL cells compared to *Rb1*$^{lox/lox}$ and POMC-Cre;*Rb1*$^{lox/lox}$*Skp2*$^{+/+}$ controls (Fig. 3a4,9,14 and d).

At 4 weeks of age, the cells in the ILs of POMC-Cre;*Rb1*$^{lox/lox}$*Skp2*$^{-/-}$ mice maintained deregulated PCNA expression and proliferation and increased apoptosis (Fig. 3b, c, and d). While the aberrantly proliferating ILs of 4 week old POMC-Cre;*Rb1*$^{lox/lox}$*Skp2*$^{+/+}$ mice had become more than 2-fold thicker than that of the *Rb1*$^{lox/lox}$ controls (Fig. 3b1,6), the proliferating yet apoptotic ILs of 4-week old POMC-Cre;*Rb1*$^{lox/lox}$*Skp2*$^{-/-}$ mice had become more than 2-fold thinner than normal (Fig. 3b11). Together, these findings indicate that *Skp2* is required for the survival of aberrantly proliferating *Rb1*-deficient melanotrophs and that *Rb1*$^{-/-}$*Skp2*$^{-/-}$ melanotroph apoptosis caused the elimination of the ILs in POMC-Cre;*Rb1*$^{lox/lox}$*Skp2*$^{-/-}$ mice.

POMC-Cre;*Rb1*$^{lox/lox}$ mice allowed us to evaluate the effect of Skp2 on p27 expression during melanotroph tumorigenesis using immunohistochemical staining (IHC). Melanotrophs of *Rb1*$^{lox/lox}$, POMC-Cre;*Rb1*$^{lox/lox}$, and POMC-Cre;*Rb1*$^{lox/lox}$*Skp2*$^{-/-}$ mice at PND 10 had comparable nuclear p27 protein stains (Fig. 3a5,10,15). However, by 4-weeks, p27 levels clearly decreased in melanotrophs of POMC-Cre;*Rb1*$^{lox/lox}$ mice (Fig. 3b10), but were maintained in the melanotrophs of POMC-Cre;*Rb1*$^{lox/lox}$*Skp2*$^{-/-}$ mice (Fig. 3b15), suggesting that *Skp2* is required for the down regulation of p27 during melanotroph tumorigenesis following *Rb1* deletion.

We next investigated how Skp2 inactivation led to the failure of p27 downregulation and whether this failure was responsible for the tumor blocking effects of Skp2 inactivation. In vitro studies have established that Skp2 mediates p27 ubiquitination in the SCF^{Skp2} ubiquitin ligase after p27 is phosphorylated on T187. However, the in vivo role of this Skp2 function has remained unclear due to divergent findings from Skp2 KO mice (in which all Skp2 functions are absent) and p27T187A KI mice (in which only Skp2's ability to mediate ubiquitination of T187-phosphorylated p27 is absent). Skp2 KO mice showed p27 protein accumulation in certain tissues and smaller body sizes [14], but p27T187A KI mice did not show p27 protein accumulation nor phenocopied Skp2 KO mice 15. Thus, in vivo, Skp2's ability to mediate ubiquitination of T187-phosphorylated p27 does not play a significant role in its ability to regulate p27. Our previous finding that pRb inhibits Skp2-mediated p27 ubiquitination by interfering with Skp2 binding to T187-phosphorylated p27 7 suggested that this Skp2 function may be deregulated and contribute to p27 protein reduction and tumorigenesis following *Rb1* loss. To evaluate this prediction, we generated POMC-Cre,$Rb1^{lox/lox}p27^{T187A/T187A}$ and the control $Rb1^{lox/lox}p27^{T187A/T187A}$ mice and examined their pituitary ILs at 4, 7, and 11 weeks of age.

The ILs of $Rb1^{lox/lox}p27^{T187A/T187A}$ mice appeared normal (Fig. 4a1), consistent with the general lack of abnormality in $p27^{T187A/T187A}$ mice. Following POMC-Cre mediated *Rb1* deletion, ILs of POMC-Cre,$Rb1^{lox/lox}p27^{T187A/T187A}$ mice at 4 weeks of age did not show the hyperplastic thickening observed in POMC-Cre,$Rb1^{lox/lox}$ mice (Fig. 3b6) but, rather, contained regional thinning (Fig. 4a2). The thinning of the IL became more wide-spread by 7 weeks of age (Fig. 4a3), and by the age of 11 weeks the entire ILs were only 2-3 cell layers thick (Fig. 4a4). The nature of the T187A KI mutation (blocking T187 phosphorylation-dependent ubiquitination of p27 by SCF^{Skp2}) predicted that the tumor blocking effects observed in $p27^{T187A/T187}$ homozygous mice should also occur in $p27^{T187A/+}$ heterozygous mice, though potentially to a smaller extent. Results shown in Fig. 4d confirm this prediction.

Similar to the effects of Skp2 KO in *Rb1*-deficient melanotrophs, p27T187A KI did not reduce the deregulated expression of PCNA and proliferation (Fig. 4a5,6,7, a9,10,11, and b), but increased apoptosis (Fig. 4a12,13,14 and c). These effects were also observed in the presence of one allele of p27T187A (Fig. 4b, c, d and data not shown). Finally, the reduced p27 expression in melanotrophs in 4-week old POMC-Cre,$Rb1^{lox/lox}$ mice (Fig. 3b10) did not occur in melanotrophs in either 4-week or 7-week old POMC-Cre,$Rb1^{lox/lox}p27^{T187A/T187A}$ mice (Fig. 4a15,16,17) nor in 7-week old POMC-Cre,$Rb1^{lox/lox}p27^{T187A/+}$ mice (data not shown). Together, these results strongly suggest that the T187 phosphorylation-dependent ubiquitination of p27 in the SCF^{Skp2} ubiquitin ligase underlies Skp2's essential role in pituitary tumorigenesis following *Rb1* loss, and that the apoptotic ablation of melanotrophs in POMC-Cre;$Rb1^{lox/lox}Skp2^{-/-}$ mice could be explained by a proapoptotic effect of p27 in these cells [16].

Notably, p27T187A KI is not equivalent to Skp2 KO because the ILs of POMC-Cre,$Rb1^{lox/lox}Skp2^{-/-}$ mice thinned to a greater degree and with faster kinetics than those in POMC-Cre,$Rb1^{lox/lox}p27^{T187A/T187A}$ mice (for example, compare Fig. 2b3,7 with Fig. 4a3,4). Skp2 has a growing list of potential substrates in addition to p27, and can support cancer cell survival by protecting cyclin A from inhibition by p27 and p21 [17], and by blocking p53 activation by p300 [18]. Further studies will be required to determine the roles of these additional mechanisms.

We next investigated whether the survival function of Skp2 revealed with mouse models was applicable to human tumors that develop due to *Rb1* mutations. As retinoblastoma is the main tumor that develops due to *Rb1*-deficiency in humans, we examined the effect of Skp2

knockdown in retinoblastoma cells. We found that knockdown of Skp2 (Fig. 5a) significantly inhibited retinoblastoma cell proliferation (Fig. 5b). Skp2 knockdown induced apoptosis, as measured by sub-G1 DNA content and TUNEL staining, but did not diminish S phase population, as measured by FACS (Fig. 5c and d). The apoptotic effects of Skp2 knockdown were evident both in the established Y79 cell line and in early passage RB177 cells.

As expected, Skp2 knockdown induced accumulation of p27 in these human retinoblastoma cells (Fig. 5e). Moreover, ectopic expression of p27 was able to inhibit proliferation and induce apoptosis (Fig. 5f-i) similar to the effects of Skp2 knockdown. Importantly, the mutant p27T187A was significantly more potent in inhibiting proliferation and inducing apoptosis, consistent with our findings from p27T187A KI mice. Restoration of pRb function largely prevented apoptosis induced either by Skp2 knockdown or by ectopic p27 expression (Fig. 5j,k), despite that the modest pRb levels slowed but did not entirely block cell proliferation (data not shown), suggesting that lack of pRb rendered the retinoblastoma cells dependent on Skp2 and sensitive to aberrantly expressed p27.

We recently showed that MDM2 plays essential roles for proliferation and survival of retinoblastoma cells and that knockdown of p14Arf diminished the requirement for MDM2 [19]. In similar experiments, we found that knockdown of p14Arf did not mitigate the effects of Skp2 knockdown, suggesting that p14Arf is not a critical target of Skp2 in these cells (Supplemental Figure 4).

Prior to the current study, inactivation of previously studied pRb targets delayed tumorigenesis in *Rb1*$^{+/-}$ mice accompanied by reduced tumor cell proliferation [1,2,3,4,5,6]. In contrast, our study reveals that inactivation of Skp2 did not reduce deregulated proliferation of *Rb1*$^{-/-}$ cells but induced apoptosis, which completely prevented tumorigenesis. Our findings add a survival arm to the pRb/E2F model of pRb function, in which pRb loss not only deregulates E2F to result in aberrant proliferation and apoptosis through various E2F target genes but also deregulates the SCF^{Skp2}-p27T187p p27 ubiquitination mechanism to down regulate p27 to provide survival support for the aberrantly proliferating pRb-deficient cells (Fig. 5l). When this mechanism is disrupted, either by inactivation of Skp2 or by blocking p27 T187 phosphorylation, the outcome of pRb loss becomes cell death, revealing that *Rb1* and *Skp2* mutations are synthetically lethal to susceptible cells. The above model predicts that Skp2 is a potentially effective drug target to prevent and treat pRb-deficient tumors. As our data suggest that the p27T187 phosphorylation-dependent function of Skp2 is required for tumorigenesis following pRb loss, yet is not needed for normal development [15], therapeutic targeting of Skp2 can focus on the p27T187-dependent function of Skp2 or p27 T187 phosphorylation.

METHODS

Mice

Rb1$^{+/-}$ mice and *Skp2*$^{+/-}$ mice have been previously described [12,14]. Mouse strain background is as follows. *Skp2*$^{+/-}$ mice on mixed C57BL/6Jx129Sv strain background were backcrossed to C57BL/6J strain mice four times, and *Rb1*$^{+/-}$ mice on mixed C57BL/6J×129Sv strain background were backcrossed to C57BL/6J mice once. *Rb1*$^{+/-}$*Skp2*$^{+/-}$ mice were then generated from these mice and were used to generate littermate *Rb1*$^{+/-}$*Skp2*$^{+/+}$ and *Rb1*$^{+/-}$*Skp2*$^{-/-}$ mice. Our *Rb1*$^{+/-}$ mice may therefore exhibit a slower tumor development kinetics than *Rb1*$^{+/-}$ mice with equal contributions from C57BL/6J and 129Sv strain background [20]. *Rb1* heterozygous mice were genotyped according to a published protocol [12]. POMC-Cre transgenic mice were genotyped as previously described [21]. Primers for

genotyping *Skp2*$^{+/-}$ mice, *Rb1*$^{lox/lox}$ mice [22], Rosa26R(YFP) mice [23], and p27T187A KI mice15 are listed in Supplemental Table 1.

The animals studied for ENU mutagenesis were C57BL/6Jx129Sv hybrid strain littermate mice from Skp2 heterozygous crosses. *Skp2*$^{+/+}$ and *Skp2*$^{-/-}$ mice were i.p. injected with ENU (0.5 mmol per gram of body weight) at PND 15±2 days as previously described [24]. Mice were sacrificed at the first sign of morbidity, which included abdominal swelling, hunched posture, and rapid breathing. Complete necropsies of all internal organs were performed including size measurement of tumors.

All mouse study protocols were approved by the Albert Einstein College of Medicine Animal Institute.

Western blot and RT-PCR analyses

Normal pituitaries, fractions of gross pituitary tumors, and fractions of ENU-induced tumors were snap frozen in ethanol-dry ice and stored in −80°C. For Western blot, frozen tissues were homogenized with Dounce glass homogenizer in tissue lysis buffer (50 mM HEPES pH7.2, 150 mM NaCl, 1 mM EDTA, 0.1% Tween-20, 1 mM DTT, and standard protease inhibitors). Tissue debris was removed by centrifugation for 10 minutes at 14,000 rpm at 4 °C. Protein concentrations of the extracts were determined by Bio-Rad protein assay kit and equal amounts of protein samples were loaded on 10% SDS gels, blotted onto PVDF membrane. Antibodies to Skp2 (H435), p27 (C-19), cyclin A (C-19), cyclin E (M-20), and Cdk2 (C-19) were from Santa Cruz Biotechnology.

For Q-PCR, tissue RNA was extracted by Trizol reagent (Invitrogen). Total RNA was treated with RQ1 DNase (Promega) at 37°C for 30 min. and RQ1 was denatured at 65°C for 20 min. T7 oligonucleotides and SuperScript II (Invitrogen) were used for the synthesis of the first strand cDNA at 42°C for 60 minutes. The PCR primers for mSkp2 and mGAPDH are listed in Supplemental Table 1. SYBR Green PCR Master Mix (4309155, ABI) and the standard program of ABI Prism 7000 were used for Q-PCR amplification.

Immunohistochemistry staining and frozen sectioning for fluorescence detection

Paraffin sections were stained with Histomouse™- plus kit (ZYMED) with antibodies to PCNA (PC10) and p27 (C-19) from Santa Cruz Biotechnology, and to BrdU (Ab-2) from Calbiochem and Ki67 as primary antibody (1 μg/ml). TUNEL staining was performed with the reagents and instructions of Apoptosis Detection Kit (S7101) from Chemicon.

Pituitaries were fixed in 4% paraformaldehyde, 10% glucose in PBS for 30 minutes and embed in Tissue Freezing Medium (H-TFM, Triangle Biomedical Sciences) on dry ice for frozen sectioning. After fluorescence photography, slides were counter-stained by Hematoxylin.

Lentivirus infection and analysis of human retinoblastoma cells

Y79 cells were purchased from the ATCC and RB177 cells were derived from a human retinoblastoma and passaged for approximately 2 months, with no evidence of a crisis phase, prior to the knockdown analyses [19]. Skp2 shRNAs were delivered by pLKO constructs TRCN0000007530 and TRCN0000007534 (Open Biosystems), and were compared to a pLKO encoding a non-silencing control shRNA (Addgene). RB177 cells with constitutive *CDKN2A*^{ARF} knockdown and pLKO-transduced controls were as described19. pRb, p27, and p27T187A were delivered using the bidirectional BE-GFP vector [25]. BE-GFP-p27+3' and BE-GFP-p27T187A+3' were produced by inserting a XmaI-XbaI fragment of pCS+p27 and pCS+p27(T187A)[26] extending from the p27 coding region to the 3' UTR between the

corresponding XmaI site and a vector XbaI site of BE-GFP-p27 25. BE-GFP-Rb was as described 25. Cells were cultured, infected, and analyzed as described19.

Statistics analysis

In the survival analysis, difference in Kaplan-Meier survival curves was analyzed by Log Rank Test (JMP software). Differences in gross tumor incidence, incidence of microscopic lesions in macroscopically normal pituitary and thyroid glands were analyzed by Fisher's exact test (MedCalc software). Differences in TUNEL labeling indices between *Rb1*$^{lox/lox}$;POMC-Cre;*Skp2*$^{+/+}$ and *Rb1*$^{lox/lox}$;POMC-Cre;*Skp2*$^{-/-}$ ILs and between *Rb1*$^{lox/lox}$;POMC-Cre;*p27*$^{+/+}$ and *Rb1*$^{lox/lox}$;POMC-Cre;*p27*$^{T187A/T187A}$ ILs were analyzed by student's *t*-test (MedCalc Software).

Supplementary Material

Refer to Web version on PubMed Central for supplementary material.

Acknowledgments

We thank J. Cui for expert technical assistance, R. Mahmood for help with tissue preparation and histological analysis, D. Abramson and S. Jhanwar for support of retinoblastoma cell analysis, A. Koff for comments on the manuscript, and A. Burns and W. Zhang for encouragement. We are grateful to T. Jacks for providing *Rb1*$^{+/-}$ mice (from L. Yamasaki, and A. Iavarone) and *Rb1*$^{lox/lox}$ mice, B. Lowell and S. Chua for POMC-Cre mice, Jim Roberts for p27T187A KI mice, and F. Costantini for Rosa26YFP mice (from J. Pollard). This work was supported by grants from the NIH-NIDDK and NIH-NCI to L.Z. Albert Einstein Comprehensive Cancer Research Center and Liver Research Center provided core facility support. L.Z. is a recipient of the Irma T. Hirschl Career Scientist Award.

References

1. Yamasaki L, et al. Loss of E2F-1 reduces tumorigenesis and extends the lifespan of Rb1($^{+/-}$)mice. Nat Genet 1998;18:360–364. [PubMed: 9537419]
2. Ziebold U, Lee EY, Bronson RT, Lees JA. E2F3 loss has opposing effects on different pRB-deficient tumors, resulting in suppression of pituitary tumors but metastasis of medullary thyroid carcinomas. Mol Cell Biol 2003;23:6542–6552. [PubMed: 12944480]
3. Lee EY, et al. E2F4 loss suppresses tumorigenesis in Rb mutant mice. Cancer Cell 2002;2:463–472. [PubMed: 12498715]
4. Lasorella A, Rothschild G, Yokota Y, Russell RG, Iavarone A. Id2 mediates tumor initiation, proliferation, and angiogenesis in Rb mutant mice. Mol Cell Biol 2005;25:3563–3574. [PubMed: 15831462]
5. Takahashi C, et al. Nras loss induces metastatic conversion of Rb1-deficient neuroendocrine thyroid tumor. Nat Genet 2006;38:118–123. [PubMed: 16369533]
6. Takahashi C, Contreras B, Bronson RT, Loda M, Ewen ME. Genetic interaction between Rb and K-ras in the control of differentiation and tumor suppression. Mol Cell Biol 2004;24:10406–10415. [PubMed: 15542848]
7. Ji P, et al. An Rb-Skp2-p27 pathway mediates acute cell cycle inhibition by Rb and is retained in a partial-penetrance Rb mutant. Mol Cell 2004;16:47–58. [PubMed: 15469821]
8. Binne UK, et al. Retinoblastoma protein and anaphase-promoting complex physically interact and functionally cooperate during cell-cycle exit. Nat Cell Biol 2007;9:225–232. [PubMed: 17187060]
9. Frescas D, Pagano M. Deregulated proteolysis by the F-box proteins SKP2 and beta-TrCP: tipping the scales of cancer. Nat Rev Cancer 2008;8:438–449. [PubMed: 18500245]
10. Zhang L, Wang C. F-box protein Skp2: a novel transcriptional target of E2F. Oncogene 2005;25:2615–2627. [PubMed: 16331253]
11. Yung Y, Walker JL, Roberts JM, Assoian RK. A Skp2 autoinduction loop and restriction point control. J Cell Biol 2007;178:741–747. [PubMed: 17724117]

12. Jacks T, et al. Effects of an Rb mutation in the mouse. Nature 1992;359:295–300. [PubMed: 1406933]
13. Vooijs M, van der Valk M, te Riele H, Berns A. Flp-mediated tissue-specific inactivation of the retinoblastoma tumor suppressor gene in the mouse. Oncogene 1998;17:1–12. [PubMed: 9671308]
14. Nakayama K, et al. Targeted disruption of Skp2 results in accumulation of cyclin E and p27(Kip1), polyploidy and centrosome overduplication. EMBO J 2000;19:2069–2081. [PubMed: 10790373]
15. Malek NP, et al. A mouse knock-in model exposes sequential proteolytic pathways that regulate p27Kip1 in G1 and S phase. Nature 2001;413:323–327. [PubMed: 11565035]
16. Carneiro C, et al. p27 deficiency desensitizes Rb-/- cells to signals that trigger apoptosis during pituitary tumor development. Oncogene 2003;22:361–369. [PubMed: 12545157]
17. Ji P, Sun D, Wang H, Bauzon F, Zhu L. Disrupting Skp2-cyclin A interaction with a blocking peptide induces selective cance cell killing. Mol Cancer Ther 2007;6:684–691. [PubMed: 17308064]
18. Kitagawa M, Lee SH, McCormick F. Skp2 Suppresses p53-Dependent Apoptosis by Inhibiting p300. Mol Cell 2008;29:217–231. [PubMed: 18243116]
19. Xu XL, et al. Retinoblastoma has properties of a cone precursor tumor and depends upon cone-specific MDM2 signaling. Cell 2009;137:1018–1031. [PubMed: 19524506]
20. Leung SW, et al. A dynamic switch in Rb+/- mediated neuroendocrine tumorigenesis. Oncogene 2004;23:3296–3307. [PubMed: 15021915]
21. Balthasar N, et al. Leptin receptor signaling in POMC neurons is required for normal body weight homeostasis. Neuron 2004;42:983–891. [PubMed: 15207242]
22. Sage J, Miller AL, Perez-Mancera PA, Wysocki JM, Jacks T. Acute mutation of retinoblastoma gene function is sufficient for cell cycle re-entry. Nature 2003;424:223–228. [PubMed: 12853964]
23. Srinivas S, et al. Cre reporter strains produced by targeted insertion of EYFP and ECFP into the ROSA26 locus. BMC Dev Biol 2001;1:4. [PubMed: 11299042]
24. Timmerbeul I, et al. Testing the importance of p27 degradation by the SCFskp2 pathway in murine models of lung and colon cancer. Proc Natl Acad Sci U S A 2006;103:14009–14014. [PubMed: 16966613]
25. Cobrinik D, Francis RO, Abramson DH, Lee TC. Rb induces a proliferative arrest and curtails Brn-2 expression in retinoblastoma cells. Mol Cancer 2006;5:72. [PubMed: 17163992]
26. Sheaff RJ, Groudine M, Gordon M, Roberts JM, Clurman BE. Cyclin E-CDK2 is a regulator of p27Kip1. Genes Dev 1997;11:1464–1478. [PubMed: 9192873]

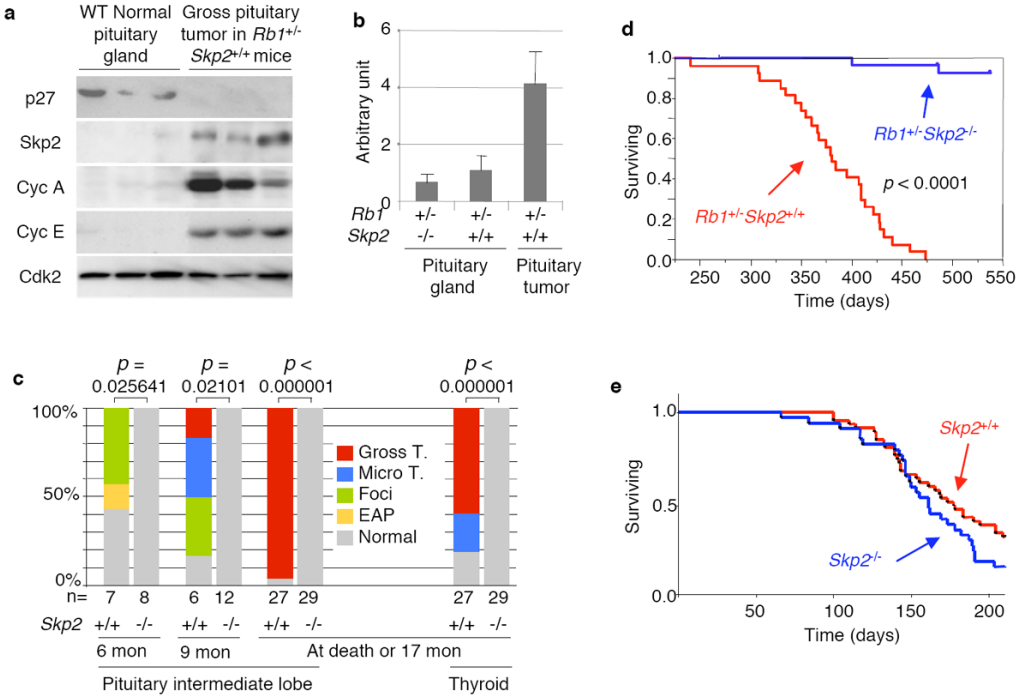

Fig. 1.

Roles of *Skp2* in spontaneous tumorigenesis in $Rb1^{+/-}$ mice and in ENU-induced tumorigenesis. **a**. Expression of the indicated proteins in wild type normal pituitary glands and pituitary tumors developed in $Rb1^{+/-}Skp2^{+/+}$ mice, determined by Western blot. **b**. Levels of Skp2 mRNA in pituitary glands and pituitary tumors (developed in $Rb1^{+/-}$ mice), determined by Q-PCR normalized with GAPDH. **c**. Incidence for pituitary and thyroid tumors at various stages in $Rb1^{+/-}Skp2^{+/+}$ and $Rb1^{-/-}Skp2^{-/-}$ mice. p values are by Fisher's exact tests (various lesions were combined for analyses). **d**. Kaplan-Meier survival analysis for the indicated mice. p value is by Log Rank test. One $Rb1^{+/-}Skp2^{-/-}$ mouse died at thirteen months and one died at sixteen months with macroscopically normal pituitary and thyroid glands. The causes of death were unclear with a possible association with eye and skin lesions. **e**. Kaplan-Meier survival analysis for the indicated mice treated with ENU.

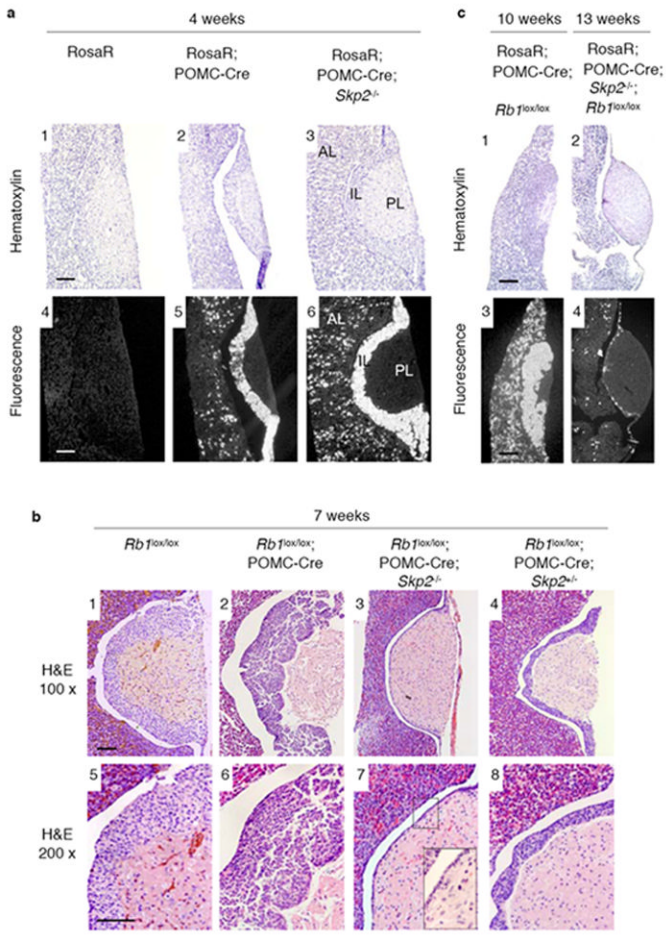

Fig. 2.

Effects of targeted deletion of *Rb1* in pituitary IL and AL of $Skp2^{+/+}$ and $Skp2^{-/-}$ mice. **a**. The POMC-Cre strain induced Cre-loxP-mediated excision in PL and AL of $Skp2^{+/+}$ and $Skp2^{-/-}$ mice. Rosa26R, Rosa26-loxP-STOP-loxP-EYFP. Mice were examined at 4 weeks of age. EYFP expression was by fluorescence of frozen-sectioned samples. **b**. Pituitary ILs of indicated mice at 7 weeks of ages. H&E stained sections of various pituitaries are shown. Big insert is enlarged view of areas marked by the small box. **c**. Pituitary glands of the indicated mice at the indicated ages, examined as in panel **a**. Scale bar, 200 μm.

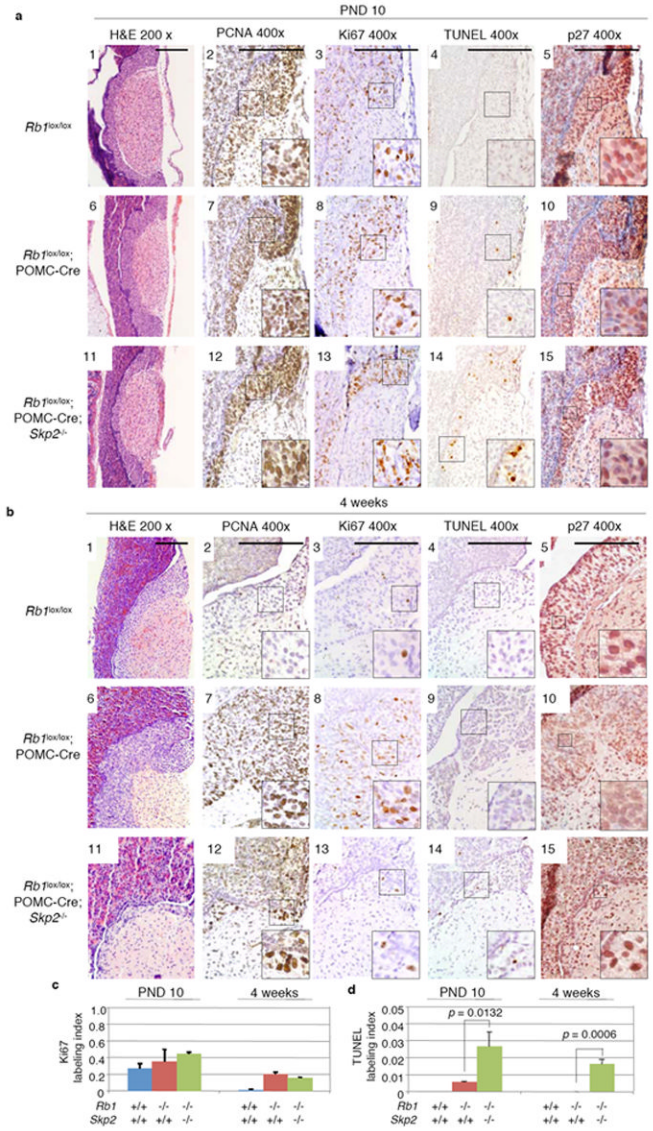

Fig. 3.

Effects of Skp2 inactivation on E2F deregulation, aberrant proliferation and apoptosis, and p27 expression in pituitary ILs following *Rb1* deletion. Various indicated mice at the ages of PND 10 (post-natal day 10) and 4 weeks are presented in panels **a** and **b**, respectively. E2F deregulation is examined by PCNA expression, proliferation by Ki67 expression, and apoptosis by TUNEL labeling. Quantification of Ki67 and TUNEL labeling in ILs was performed with three pituitaries of each indicated genotypes at the indicated ages. *Rb1* genotypes indicate the outcome of Cre-loxP mediated deletion in IL. p values are by *t* test. Error bars are s.d. Scale bar, 200 μm.

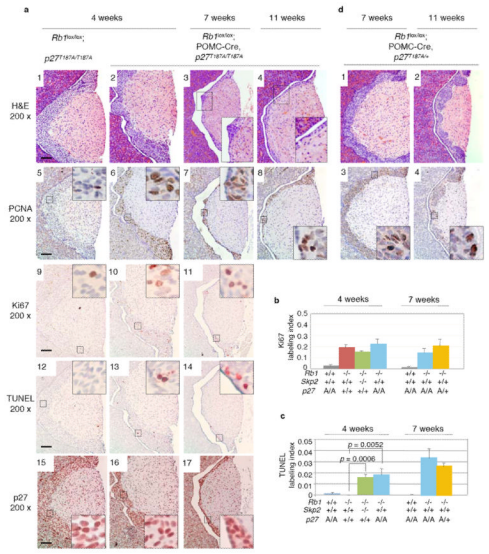

Fig. 4.

Effects of targeted deletion of *Rb1* in pituitary IL of p27T187A KI mice. **a**. IL morphology, PCNA expression, Ki67 and TUNEL labeling, and p27 expression were examined at the indicated ages, with quantification of Ki67 and TUNEL labeling presented in **b** and **c**, respectively. p values are by *t* test. Error bars are s.d. **d**. IL morphology and PCNA expression after *Rb1* deletion in $p27^{T187A/+}$ mice at 7 and 11 weeks of age. Scale bar, 200 μm.

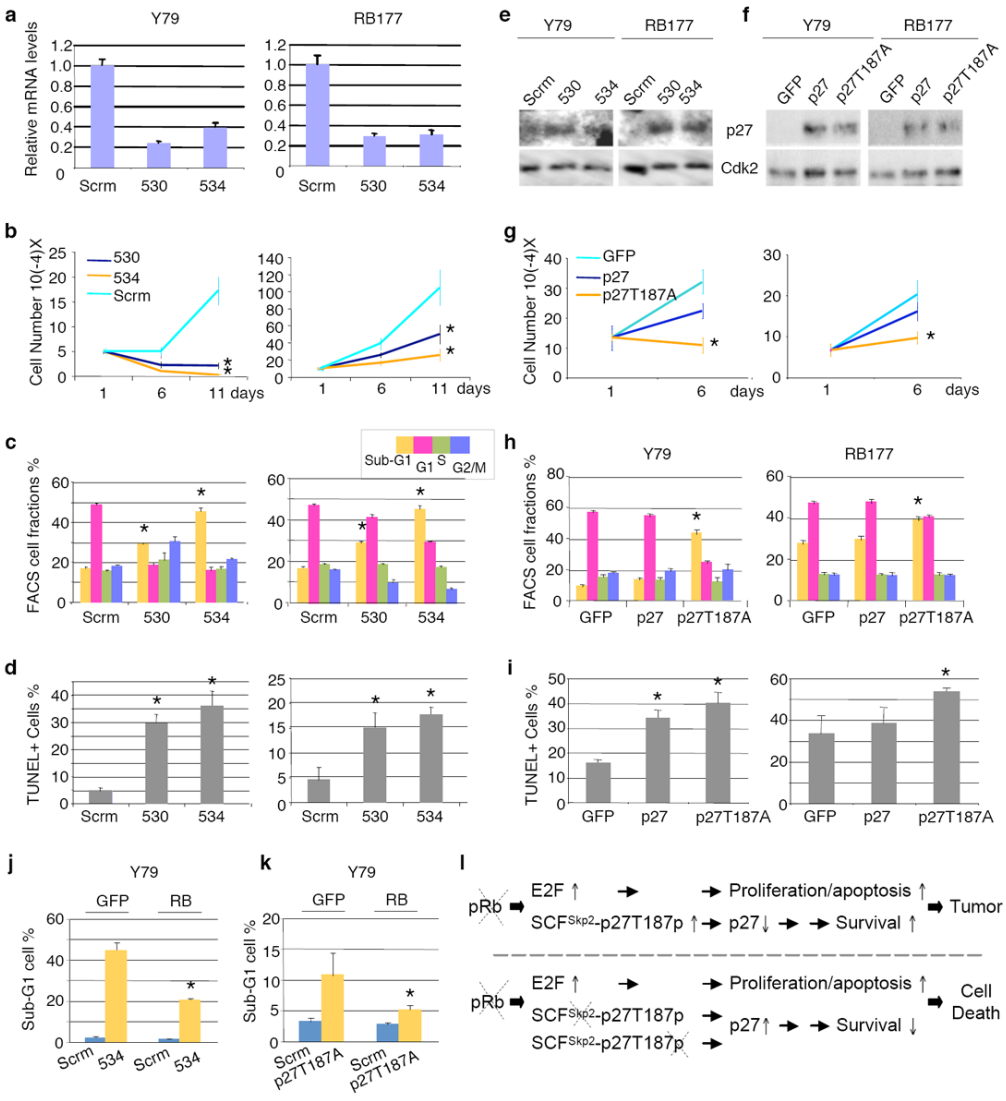

Fig. 5.

Effects of Skp2 knockdown and stabilized p27 expression on established Y79 cells and early passage RB177 retinoblastoma cells. (**a-e**) Y79 and RB177 cells infected with lentiviruses expressing shRNA targeting Skp2. Two independent Skp2 shRNAs and a scrambled shRNA control (Scrm) were used as indicated. After drug selection, infected cells were evaluated for Skp2 mRNA by quantitative RT-PCR (**a**), cell proliferation by counting live cells (**b**), cell cycle profile by FACS (**c**), apoptosis by TUNEL staining (**d**), and p27 expression by Western immunoblotting, with Cdk2 as a loading control (**e**). (**f-i**) Y79 and RB177 cells infected with BE-GFP lentiviral vector encoding p27 or p27T187A. Infected cells were evaluated for p27 expression (**f**), cell proliferation (**g**), cell cycle profile (**h**), and TUNEL staining (**i**), (**j-k**) Y79 cells transduced with BE-GFP vector or BE-GFP-RB, followed 2 days later by transduction with *Skp2* shRNA or scrambled shRNA control (**j**) or with BE-GFP or BE-GFP-p27T187A (**k**), and evaluated cells with sub-G1 DNA content. Averages with s.d. are shown. Asterisks indicate $P < 0.05$ relative to applicable controls. **l**. A new model of tumorigenesis after *Rb1* loss. Two consecutive arrows suggest the presence of multiple steps between them.